Received 3 July 2025; Accepted 5 November 2025
https://doi.org/10.48612/letters/2025-4-369-375

https://elibrary.ru/jihdvp

Temperature dependence of friction and wear in nanostructured shape memory alloy $Ti_{49.3}Ni_{50.7}$

A. A. Dmitrievskiy†[1], V. V. Stolyarov[2]

†aadmitr@yandex.ru

[1]Derzhavin Tambov State University, Tambov 392026, Russia
[2]Mechanical Engineering Research Institute of the Russian Academy of Sciences, Moscow 101000, Russia

Abstract: The temperature dependence of friction and wear of nanostructured alloy $Ti_{49.3}Ni_{50.7}$ obtained by severe plastic deformation is investigated. The friction coefficient (K_f) and wear rate (W) are investigated under conditions of reciprocating motion and the absence of lubrication in the temperature range ($25°C \le T \le 140°C$) corresponding to two-phase (A+M) and single-phase (A) states. It is shown that the minimum friction conditions in the range ensure the absence of a temperature flash in the contact area and allow us to state that the friction coefficient, wear intensity and volume lost by the counterbody linear increase with temperature change in the range of 25 – 90°C and are drawn on a plateau at temperature M_d. With an increase in the tribocontact temperature, the running-in stage is reduced. The change in friction characteristics is associated with the ratio of martensite and austenite content.

Keywords: titanium nickelide, shape memory alloy, martensite, friction coefficient, wear

Acknowledgements: *The work was carried out using funds from the State Assignment, scientific topic code assigned by the founder (organization) FFGU-2024-0023. The authors thank the employees of the plastic deformation laboratory of the IMET RAS for providing the research samples. The research was carried out using the equipment of the Center for Collective Use of Scientific Equipment of Derzhavin Tambov State University.*

1. Introduction

The results of experimental and computer modeling indicate that the initial microstructure of the alloys (grain size, phase composition, dislocation density, type of crystal lattice) and external conditions (environment, temperature, surface roughness) have a strong effect on the physical and mechanical properties of the materials, including wear resistance and friction coefficient [1, 2]. Moreover, structural changes in the surface layer (phase transitions, recrystallization, amorphization, refinement) caused by plastic deformation during friction can significantly affect the hardness and, accordingly, the tribological behavior of the material.

This aspect was studied in the TiNi alloy, which undergoes martensitic transformation under the action of external loads or temperature [3]. The unique properties of superelasticity and shape memory of TiNi alloys are the basis for their wide functional application, for example, in sealants, drives and the biomedical industry [4, 5]. Moreover, TiNi shape memory alloys have high strength and plasticity and are therefore promising structural materials. Relatively recently, it became known that such alloys have increased wear resistance compared to other high-strength materials [6 – 8]. Moreover, wear and friction coefficient are structure-sensitive properties to grain size or the ratio of austenitic and martensitic phases. Therefore, tribological studies were investigated in both martensitic and austenitic states [6]. Even though detailed experimental data on friction and wear in TiNi are available in the literature [6 –10], the physical reason for the increased wear resistance has not been established due to the complexity of the deformation behavior and temperature-dependent reversible phase transformation [11–13]. As for the effect of temperature on the tribological behavior of the TiNi alloy, almost all the literature data refer to the coarse-grained state of the alloy [6 – 9]. The first studies on the effect of grain size on the friction coefficient in the TiNi alloy processed by cold rolling with a pulsed current were presented in [10]. However, the measurements were performed with current heating in such a wide temperature range of 20 – 800°C that detailed data in the low-temperature (<150°C) region were not available. Recently, the results of molecular dynamics simulations of the temperature effect on friction during nanoscratching in a single crystal TiNi alloy were published [14]. The critical role of the start transformation temperature A_S is demonstrated. With increasing temperature in the region $T < A_S$, the friction coefficient K_f decreases, and at $T > A_S$, on the contrary, it increases. For a correct analysis of the temperature dependence of friction in TiNi alloys, it is important to keep in mind the existence of another important temperature M_d (the maximum temperature of martensite formation under load), information about which is quite rare.

Thus, the temperature factor and its relationship with friction characteristics in the region close to phase transformations temperature remains insufficiently studied. In this regard, the aim of the work was to establish the

temperature dependence of the friction coefficient and wear rate in the ultrafine-grained TiNi shape memory alloy.

2. Materials and methods

The material for the study was the $Ti_{49.3}Ni_{50.7}$ alloy in the form of a rod with a diameter of 3.5 mm. To form a nanostructure, the alloy was subjected to severe plastic deformation by screw rolling and rotary forging. More detailed information concerning processing conditions and microstructure can be found in [15]. The average grain size in the alloy microstructure was 60 – 80 nm. Table 1 presents the temperatures of martensite transformations during heating/cooling of the $Ti_{49.3}Ni_{50.7}$ alloy, corresponding to the beginning (R_S) and end (M_f) of the direct transformation, the beginning (A_S) and end (A_f) of the reverse transformation, as well as the temperatures of the corresponding peaks (T_{max}). Based on the DSC results, at room temperature all three main phases B2 austenite, R and B19' martensite are present in the alloy [15].

Table 1. Transformation temperatures (°C) in nanostructured $Ti_{49.3}Ni_{50.7}$ alloy.

M_f	T_{max}	R_S	A_S	T_{max}	A_f
−67	35	56	10	25	63
← When cooling			When heated →		

For tribological tests, half-cylinders measuring 20 × 3.5 mm were cut from the original rod by electric spark cutting. These half-cylinders were pressed into thermoplastic, ground and polished to a surface roughness of R_a=150 ± 50 nm.

Tribological tests were performed on a TRB3 tribometer (Anton Paar, Austria). The mode of reciprocating motion of the counterbody according to the "ball-plane" scheme without lubrication at a normal load of F = 0.2 N was used. The counterbody was a ball made of Al_2O_3 ceramics, 1.5 mm in diameter. The speed and amplitude of the sample motion relative to the stationary ball were 2 cm/s and 5 mm, respectively. Friction and wear tests were carried out at several temperatures in the range from room temperature to T=140°C. For this purpose, the tribo-pair (sample-ball) was continuously blown with an airflow of a given (elevated) temperature. The temperature of the tribo-pair during the tests was controlled using a thermocouple brought into rigid mechanical contact with the sample. Additionally, the sample temperature was controlled using a Testo 875-1i thermal imager (Testo, Germany). The accuracy of measuring the temperature of the tribocontact using a thermocouple and a thermal imager was ±2°C and ±0.1°C, respectively.

In all wear tests, the number of friction cycles was kept constant: N = 3000. With a track length of 10 mm, this provided a total travelled distance of L=60 m. The friction coefficient K_f was recorded throughout the test. The wear rate W was calculated using the equation recommended by ASTM G133:

$$W = \frac{V}{F \times L},$$

where V is the volume of removed material (mm^3), calculated as the product of the track length and its cross-sectional area, which was determined using a profilometer (Wyko NT9080, Germany). Each point on the graphs of the $K_f(T)$ and $W(T)$ dependencies is an average of at least 8 individual measurements.

3. Results

3.1. Tribocontact temperature (without external heating)

In the tribocontact zone, at high sliding speeds and pressing forces of the test sample and the counterbody, the temperature can increase significantly (by tens and even hundreds of degrees) (the so-called flash temperature). This can be equivalent to increasing the temperature to which the test sample is deliberately heated from an external heat source. For the ball-plane tribocontact, the flash temperature in the contact zone can be estimated from the relationship [16]:

$$\Delta T = \frac{8K_f F v}{3\pi^2 a(k_b + k_p)},$$

where K_f is the friction coefficient, F is the clamping force, v is the speed of relative movement of the counterbody (in the form of a ball) and the flat sample, k_b and k_p are the thermal conductivities of the ball and sample, respectively, a is the radius of the contact zone, which, in accordance with [17], can be calculated from the equation:

$$a = \left(\frac{3FR_b}{4E^*}\right)^{\frac{1}{3}},$$

where R_b is the radius of the spherical counterbody, E^* is the reduced modulus of elasticity.

Possible increase in temperature ΔT in the contact zone under identical friction conditions of a TiNi specimen and a counterbody in the form of an Al_2O_3 ball was calculated in [15]. The calculation showed that under the used comparatively low speeds v and loads F, the value of ΔT = 2.15°C and is comparable with ambient temperature fluctuations. Infrared images were recorded to experimentally confirm the obtained estimate of ΔT during friction (at the running-in stage and at the steady-state wear stage). As an example, Fig. 1 shows an infrared image of a friction pair and histograms of temperature distribution along a line normally intersecting the wear track being formed (at room temperature). The recorded data at the initial stage of friction (100 –150 cycles of reciprocating motion of the friction pair), which, as will be shown below, should be attributed to the running-in stage, and at a later stage of wear (2000 cycles) — to the steady-state wear stage.

It is evident that at the running-in stage the contact area does have a slightly higher temperature. However, the difference between the temperature of the main volume of the sample and the ambient temperature ΔT does not exceed 2.5°C, which is fully consistent with the calculated value ΔT = 2.15°C [15]. At the wear stage, corresponding to 2000 cycles, the experimentally determined temperature difference ΔT does not exceed 0.5°C. Thus, it is shown that under the experimental conditions used, the flash temperature cannot affect possible changes in the tribological

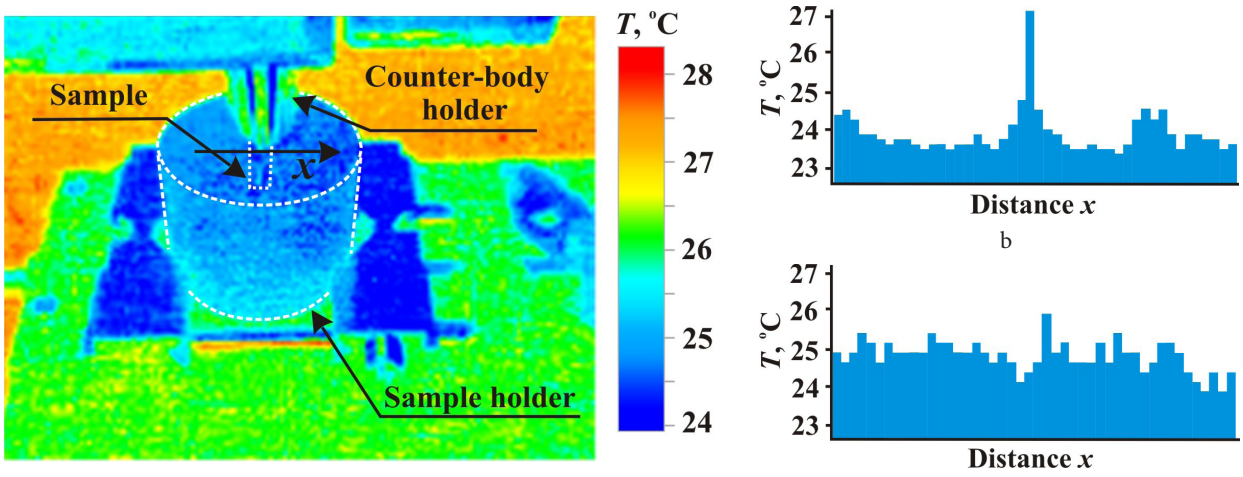

Fig. 1. (Color online) Infrared image of a friction pair (a) and histograms of temperature distribution along a line normally intersecting the formed wear track, recorded at the running-in stage (b) and at the stage of steady wear (c).

characteristics of the TiNi alloy with an increase in the test temperature (of the entire sample from an external heat source) even by several tens of degrees.

3.2. Effect of heating from an external source on the friction coefficient

The dependences of the friction coefficient on the number of cycles during the reciprocating motion of the friction pair $K_f(N)$ were recorded at different temperatures (in the range $25°C \le T \le 140°C$). As an example, Fig. 2 shows the dependences $K_f(N)$ recorded at temperatures of 25°C, 70°C, 90°C and 140°C.

It is known that at the beginning of the test, the highest unevenness of the friction pair surfaces are the first to contact. In this case, overestimated K_f values and the most intense wear are observed. This stage is called the running-in period or stage. As follows from the data presented in Fig. 2, the running-in stage at room temperature (curve 1) lasts about 750 cycles. An increase in the test temperature helps to reduce the number of cycles required for running-in of the rubbing surfaces (Fig. 2, curves 2 and 3, respectively). As the number of wear cycles increases, the rubbing surfaces are smoothed out (adapted to each other), the wear process, as a rule, stabilizes, and the running-in stage is replaced by the stage of steady-state wear. A comparative analysis of the $K_f(N)$ dependencies at the stage of steady-state wear (Fig. 2) clearly demonstrates that an increase in temperature from room temperature to $T = 70°C$ leads to a significant increase in the friction coefficient. A further increase in temperature (up to $T = 140°C$) does not cause changes in K_f (taking into account the measurement error). The numerical value of the friction coefficient is determined by averaging the data at the steady-state wear stage. Figure 3 shows the dependence of the friction coefficient (calculated at the steady-state wear stage) on temperature. It is evident that in the temperature range of $25°C \le T \le 70°C$, the friction coefficient increases linearly from 0.57 to 0.78. A further increase in the test temperature (up to $T = 140°C$) is accompanied by a slight decrease in K_f reaching a plateau (at $T \ge 120°C$ $K_f = 0.73$).

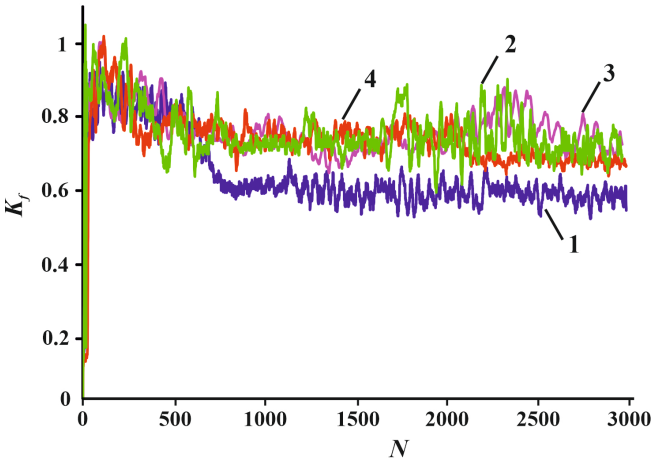

Fig. 2. (Color online) Dependences of the friction coefficient on the number of cycles, recorded at temperatures: 1 — 25°C; 2 — 70°C; 3 — 90°C, 4 — 140°C.

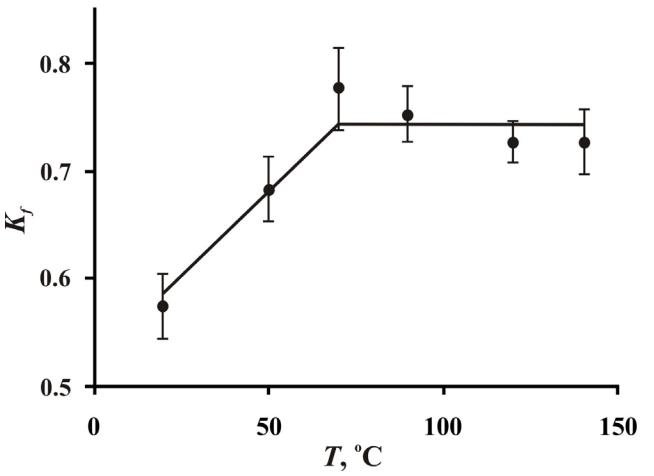

Fig. 3. Dependence of the friction coefficient K_f on the test temperature T.

3.3. Effect of heating from an external source on wear rate

A wear track is formed during friction. It was found that the volume of removed material (at the maximum number of cycles $N = 3000$) depends on the test temperature. Thus, Fig. 4 a, b show 3D profilograms of wear tracks formed during friction at temperatures $T = 25$°C and $T = 140$°C, respectively, as an example. It is evident that the high-temperature track is more than one and a half times wider and almost twice as deep as the track formed at room temperature.

Quantitative analysis of wear track profilograms allows calculating wear rate. The dependence of wear rate W on test temperature T is shown in Fig. 4 c (curve 1). It is evident that with an increase in test temperature from room temperature to 90°C, wear rate increases, and in the temperature range $90°C \le T \le 140°C$, wear rate remains unchanged, taking into account the measurement error. That is, the dependence $W(T)$ is qualitatively similar to the dependence $K_f(T)$.

The dependence of the volume lost by the counterbody (Al_2O_3 sphere) on the number of cycles $V_b(N)$, shown in Fig. 4 c (curve 2), is qualitatively similar. That is, an increase in the test temperature from room temperature to 90°C causes an almost fivefold increase in the wear of the counterbody. However, a further increase in temperature (by another 50°C) does not lead to an increase in V_b noticeable taking into account the measurement error. The qualitative similarity of the dependencies $K_f(T)$, $W(T)$ and $V_b(T)$, expressed in their "inflection" in the test temperature range $T_C \approx 70 - 90$°C, indicates a change in the wear mechanism in this temperature range.

4. Discussion

Titanium nickelide is a complex object in which the structural and phase state depends on both temperature and stress (strain). When heated in the range of 25 – 140°C even without external stress, a reversible martensitic transformation occurs in it with an increase in the volume fraction of austenite to 100%. Since the friction process can result in additional structure refinement of the surface layers, plastic deformation and acts mechanical stresses, these factors can shift the intervals of martensitic transformation (in particular the transformation of B2 → R) by tens of degrees towards higher temperatures [18]. As a result, external conditions (temperature and normal pressure of the counterbody) during friction are significant when measuring the friction coefficient and wear resistance. In addition, the alloy under study should be considered as an elastomer that exhibits superelasticity and shape memory properties, as well as a composite in which there is a hard matrix (austenite) and relatively soft inclusions (martensite). It should also be noted that due to the very different hardness of the Al_2O_3 counterbody (tens of GPa) and titanium nickelide (units of GPa), the main wear mechanism is abrasive wear. For the same reason, despite the low roughness of the contact surfaces ($R_a \approx 0.1$ μm), adhesive wear is absent [19].

The dependences of the friction coefficient on the number of cycles for all the studied temperatures in the range of 25 – 140°C have a typical appearance and indicate the presence of a maximum and minimum friction coefficient, respectively, at the running-in stage and the steady-state stage (Fig. 2). It is known that the maximum and minimum of the friction coefficient correspond to static friction (static, elastic deformations) and sliding friction (kinetic, plastic deformations) [20], while the static friction coefficient has no practical significance. In this regard, when assessing the temperature dependence of the friction coefficient of titanium nickelide, the values at the steady-state stage will be taken into account. For both stages, the friction process can be considered isothermal, due to an insignificant, less than 2.5°C, increase in the tribocontact temperature (flash temperature) (Fig. 1).

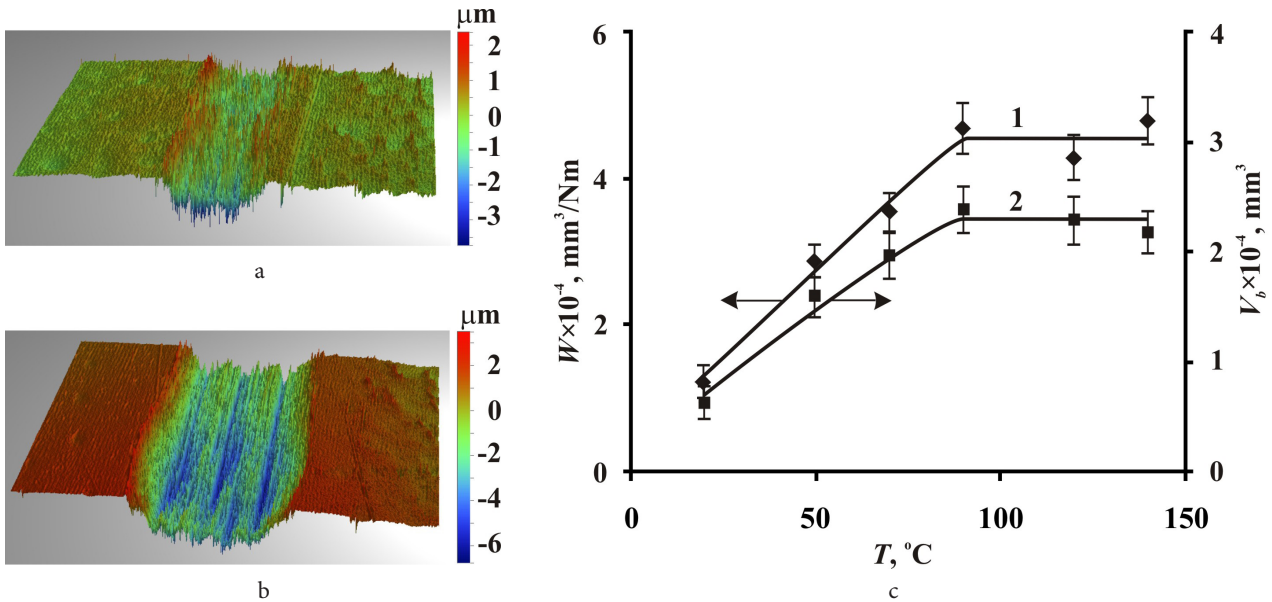

Fig. 4. (Color online) 3D profilograms of wear tracks formed during friction at test temperatures $T = 25$°C (a) and $T = 140$°C (b), as well as the dependence of wear rate W (curve 1) and volume lost by the counterbody V_b (curve 2) on test temperature T (c).

4.1. Friction and wear rate at room temperature

Tribological tests have shown that the friction coefficient (Fig. 3) and the wear rate value (Fig. 4c, curve 1) of the studied alloy at room temperature and at the steady-state stage are the lowest. In accordance with the structural and DSC data [15] the nanostructured $Ti_{49.3}Ni_{50.7}$ alloy at room temperature (before tribological tests) is in a three-phase (M + R + A) state, in which the predominant phase is austenite. However, during friction the ratio of the volume fractions of the phases apparently changes.

Indeed, under conditions of isothermal friction the main influence on the phase composition can only be exerted by mechanical stress and the accompanying plastic deformation. Since both shift the temperature range of martensitic transformation to a larger side, it can be assumed that during friction at room temperature the contribution of the martensite phase will increase and become preferential compared to the austenite. It is well known that the deformation of TiNi alloy in the martensitic state proceeds through the stages of elastic deformation, martensite reorientation, elastic deformation of reoriented martensite and "dislocation" plastic deformation of reoriented martensite. Thus, we assume that the main deformation mechanism during the reciprocating motion of the counterbody is the elastic deformation of detwinned martensite. In addition, at room temperature, a certain contribution is made by the superelastic behavior of austenite. This combination of deformation mechanisms in the contact area of the friction pair provides the lowest friction coefficient and wear intensity observed in our experiment. Note that because of the change in the phase composition of the TiNi alloy, the deformation mechanisms involved in the friction and wear process become temperature dependent.

4.2. Friction and wear rate at 25°C < T < 70°C

An increase the tribocontact temperature from an external source (to 70°C) promotes thermally stimulated R→B2 transformation, i.e. redistribution of the relative shares of the martensite (R) and austenite (B2) phases. This is accompanied by a significant increase in the friction coefficient, wear rate and volume lost by the counterbody (Fig. 3 and Fig. 4), which is obviously caused by an increase in the austenite (B2) fraction. That is, in the temperature range of 25°C < T < 70°C, the contribution of the martensite phase (R) of the TiNi alloy gradually decreases and the role of the austenite (B2) phase in the deformation of the alloy during friction increases. It should be noted that the deformation of TiNi alloy in the austenitic metastable state (at $T < M_d$) proceeds through the stages of elastic deformation of austenite (B2), martensitic transformation R-B2 under load, elastic deformation and "dislocation" plastic deformation of stress-induced martensite (R).

4.3. Friction and wear rate at 70°C ≤ T ≤ 90°C

As can be seen from Fig. 3 and Fig. 4, in the temperature range 70°C ≤ T ≤ 90°C, inflections are observed in the temperature dependences of the friction coefficient (at the temperature $T \approx 70$°C), wear rate and volume lost by the counterbody (at the temperature $T \approx 90$°C). This may be the result of the complete disappearance of the "low-temperature" martensite fraction of the TiNi alloy. That is, in the contact zone of the friction pair, deformation of the metastable austenite phase can be realized through a sequence of stages described earlier.

It should be noted that in the temperature range under consideration, an extremum (minimum) is observed in the temperature dependence of the elastic modulus of TiNi alloys [21] and, as a consequence, in the temperature dependence of the average contact stresses in the friction pair σ_H. This, in turn, can affect the ratio of σ_H and critical stresses causing mechanically induced A→M transformations and lead to a change in the dominant wear mechanism. We will return to the discussion of this issue below.

4.4. Friction and wear rate at T > 90°C

At temperatures above 90°C the temperature dependences of the wear rate, volume lost by the counterbody and especially friction coefficient, transform into a plateau (Fig. 3 and Fig. 4). Apparently, this is the result of the termination of thermally and mechanically induced martensitic transformations in the contact area of the friction pair. At the same time, it is known that at temperatures above M_d, the deformation of the TiNi alloy occurs due to elastic deformation, and then "dislocation" plasticity of stable austenite. Based on this, it can be assumed that for the nanostructured $Ti_{49.3}Ni_{50.7}$ alloy $M_d \approx 90$°C.

4.5. Ratio of average contact and critical stresses

The friction coefficient and wear intensity depend on the ratio of elastic and plastic deformation of the material in the contact zone of the friction pair. This ratio, in turn, depends on the ratios of the average contact stresses in the friction pair σ_H and the critical stresses causing phase transformations or dislocation plasticity. In this regard, the elastic deformation in the contact zone of the friction pair can dominate if σ_H does not exceed the stress causing martensite reorientation at T < 70°C ($\sigma_H < \sigma_{re}^M$), or the dislocation yield stress of martensite at T < 70°C ($\sigma_H < \sigma_y^M$), or the critical stress inducing martensite transformation for the austenitic state at T < 90°C ($\sigma_H < \sigma_{A\text{-}M}$), as well as the critical stress causing dislocation plasticity of austenite at $T > M_d$. Otherwise, that is, when $\sigma_H > \sigma_y^M$, or $\sigma_H > \sigma_{re}^M$ at T < 70°C, or $\sigma_H > \sigma_{A\text{-}M}$ at T < 90°C, and also if the average contact stresses are capable of causing dislocation plasticity at $T > M_d$, then plastic deformation dominates. An increase in the role of plastic deformation in the tribocontact zone is accompanied by an increase in the friction coefficient and wear intensity [8].

To estimate the average contact stress in the ball-plane system, according to [8], the following equation was used:

$$\sigma_H = \sqrt[3]{\frac{6F\left(E^*\right)^2}{\pi^3 r^2}},$$

where E^* is the reduced elastic modulus, r is the radius of the sphere (counterbody). The reduced elastic modulus E^* was calculated from the known equation:

$$\frac{1}{E^*} = \frac{1-\nu_b^2}{E_b} + \frac{1-\nu_p^2}{E_p},$$

where ν_b, ν_p, E_b and E_p are Poisson's ratios and elastic modules of the spherical counterbody and flat sample, respectively.

Using the known data on Poisson's ratios and elastic modules of TiNi alloys and Al_2O_3, for example, [17,22,23], it is not difficult to calculate the contact stress σ_H. For room temperature $\sigma_H = 0.67$ GPa.

As shown in [21,24] the elastic modulus of TiNi alloys decreases by approximately 10% with an increase in temperature from room temperature to 70–80°C and then increases by 10–15% (relative to room temperature) with an increase in temperature to 120–150°C. Such thermally induced changes in the elastic modulus cause corresponding changes in the average contact stresses σ_H: a decrease to values of ≈0.63 GPa, and then, conversely, an increase to values of ≈0.73 GPa.

It should be noted that, according to [24], the transformation yield stress and critical stress for martensite reorientation decrease in a similar way, when the M_S is approached from the higher or from the lower temperatures. In the temperature range $A_S < T < M_d$, the critical stresses of martensite transformations $\sigma_{A\text{-}M}$ increase. At $T > M_d$, a decrease in the true yield stress is observed [24].

Thus, the decrease in average contact stresses in the temperature range from room temperature to 70–80°C (caused by a decrease in the elastic modulus) correlates with a decrease in the critical stresses of martensite reorientation σ_{re}^{M} at $T < M_S$. The increase in average contact stresses at $T > 70–80$°C (caused by an increase in the elastic modulus) correlates with the temperature dependence of the critical stresses of martensite transformations $\sigma_{A\text{-}M}(T)$ in the temperature range $M_S < T < M_d$. That is, in the entire temperature range from room temperature to M_d, the ratios of average contact stresses in the tribo-pair and critical stresses σ_y^M, σ_{re}^M and $\sigma_{A\text{-}M}$ should not change significantly. In this regard, an increase in the test temperature up to M_d should not cause a change in the dominant wear mechanism. Indeed, as follows from the data presented in Fig. 3 and Fig. 4, the friction coefficient, wear rate and volume lost by the ball increase monotonically with an increase in temperature from room temperature to 70–90°C. The growth of the listed characteristics in the temperature range 25°C < T < 70°C should therefore be associated with a gradual redistribution of phases as the temperature increases: a decrease in the relative proportion of the R-phase (B19'-martensite) and an equivalent increase in austenite.

The plateau of temperature dependences of the friction coefficient, wear rate and volume lost by the counterbody observed at $T > 90$°C is obviously associated with the temperature exceeding M_d. As noted above, at $T > M_d$ martensite is not formed under load and, consequently, the component of plastic deformation in the contact area of the friction pair associated with the plastic deformation of mechanically induced martensite disappears. A decrease in the contribution of plastic deformation to the wear mechanism helps to reduce the friction coefficient and wear rate and, as a consequence, the volume lost by the counterbody.

4. Conclusions

The paper studies the regularities of the friction coefficient and wear rate changes for $Ti_{49.3}Ni_{50.7}$ alloy in the nanostructured state (grain size 60–80 nm) under dry friction against a spherical counterbody made of Al_2O_3 in the temperature range of 25°C < T < 140°C. It has been established that the thermo mechanically induced phase transformation of TiNi alloy (the ratio of relative proportions of B2-austenite, R-phase and/or B19'-martensite) play a decisive role in changing the above tribological characteristics. The conducted studies allowed us to draw the following conclusions:

1. The absence of a significant temperature flash in the contact area of the tribo-pair ($Ti_{49.3}Ni_{50.7}$ alloy — counterbody made of Al_2O_3) at a relative motion speed of 2 cm/s and a clamping force of 0.2 N has been experimentally proven.
2. It has been shown that an increase in the temperature of the tribo-pair from an external heat source helps to reduce its running-in stage.
3. A qualitative similarity of the temperature dependences of the friction coefficient, wear rate of the $Ti_{49.3}Ni_{50.7}$ alloy and the volume lost by the counterbody has been revealed. The specified characteristics increase linearly with increasing temperature in the range of 25°C < T < 70°C. At $T > 90$°C, the specified dependences reach a plateau.
4. It was found that the thermally induced increase in the friction coefficient K_f and wear intensity W of $Ti_{49.3}Ni_{50.7}$ alloy in different temperature ranges is due to different reasons. In the range of 25°C < T < 70°C, the increase in K_f and W is caused by an increase in the volume fraction of austenite compared to martensite.
5. A joint analysis of the temperature dependences of the phase composition, friction coefficient and wear rate allowed us to conclude that in nanostructured $Ti_{49.3}Ni_{50.7}$ alloy, the temperature of the austenite transition to a stable state (not transformed into martensite under load) has a value of $M_d \approx 90$°C.

References

1. P.N. Khopin, S.V. Shishkin, Tribology: a textbook for universities, Moscow, Yurait, 2025, 236 p. (in Russian)
2. S. Cheng, M. Chandross, Atomic Origins of Friction Reduction in Metal Alloys, Tribol. Lett. 69 (2021) 69.
3. R. Yang, W. Ma, Ch. Duan, Z. Yang, Y. Zhang, T. Wang, Q. Wang, Tribologically induced amorphization in the subsurface of aged Ni-rich TiNi alloy during dry sliding, Intermetallics. 113 (2019) 106574.
4. K. Zadafiya, S. Kumari, S. Chatterjee, K. Abhishek, Recent trends in non-traditional machining of shape memory alloys (SMAs): a review, CIRP J. Manuf. Sci. Technol. 32 (2021) 217–227.
5. J. Zhu, Q. Zeng, T. Fu, An updated review on TiNi alloy for biomedical applications, Corrosion Rev. 37 (6) (2019) 539–552.
6. J.X. Liu, S.B. Sun, F. Chen, Y.X. Tong, L. Guan, High temperature wear behavior of Ni-rich NiTi-based alloys. J. Mater. Res. Technol. 20 (2022) 440–447.
7. I. Ben Naceur, K. Elleuch, Tribological properties of deflected NiTi superelastic archwire using a new experimental set-up: Stress-induced martensitic transformation effect, Tribol. Int. 146 (2020) 106033.
8. A. Avcil, A.A. Eker, B.O. Kucukyildirim, Influence of sliding rate and load with friction on NiTi shape memory alloy wear resistance, Met. Sci. Heat Treat. 64 (2022) 211–218.

9. N. Levintant-Zayonts, G. Starzynski, M. Kopec, S. Kucharski, Characterization of NiTi SMA in its unusual behaviour in wear tests, Tribology Int. 137 (2019) 313 – 323.
10. A. A. Misochenko, S. V. Chertovskikh, L. S. Shuster, V. V. Stolyarov, Influence of grain size and contact temperature on the tribological behaviour of shape memory $Ti_{49.3}Ni_{50.7}$ alloy, Tribol. Lett. 65 (2017) 131.
11. Y. Q. Zhang, S. Y. Jiang, L. Hu, Y. L. Liang, Deformation mechanism of NiTi shape memory alloy subjected to severe plastic deformation at low temperature, Mat. Sci. Eng. A-Struct. 559 (2013) 607 – 614.
12. Y. Zhang, S. Jiang, G. Zhao, K. Guo, Transformation yield surface of nanocrystalline NiTi shape memory alloy, Int. J. Mech. Sci. 222 (2022) 107258.
13. B. Li, Y. Shen, Q. An, Structural origin of reversible martensitic transformation and reversible twinning in NiTi shape memory alloy, Acta Mater. 199 (2020) 240 – 452.
14. X. Chen, A. Guo, J. Wang, S. Lu, T. Fu, Temperature dependence of tribological properties in NiTi shape memory alloy: A nanoscratching study, Tribology International 197 (2024) 109812.
15. A. Dmitrievskiy, V. Komarov, R. Karelin, V. Andreev, V. Stolyarov, Friction and Wear Resistance of Nanostructured TiNi Shape Memory Alloy, Metals 14 (2024) 1248.
16. M. L. Rahaman, Liangchi Zhang, On the estimation of interface temperature during contact sliding of bulk metallic glass, Wear 320 (2014) 77 – 86.
17. A. Kasperski, A. Weibel, D. Alkattan, C. Estournès, V. Turq, Ch. Laurent, A. Peigney, Microhardness and friction coefficient of multi-walled carbon nanotube-yttria-stabilized ZrO_2 composites prepared by spark plasma sintering, Scripta Materialia 69 (2013) 338 – 341.
18. Ch. Jiang, H. Xu, Effect of Pre-Deformation on the Transformation Temperatures of TiNi Shape-Memory Alloys, Materials Science Forum, 394 – 395 (2002) 269 – 272.
19. V. L. Popov, Mechanics of contact interaction and physics of friction. From nanotribology to earthquake dynamics, Moscow, FIZMATLIT, 2013, 352 p. (in Russian)
20. N. S. Penkin, A. N. Penkin, V. M. Serbin, Fundamentals of Tribology and Tribotechnics. Textbook for Universities, Moscow, Mechanical Engineering, 2021, 208 p. (in Russian)
21. S. Spinner, A. G. Rozner, Elastic properties of NiTi as a function of temperature, The Journal of Acoustic Society of America 40 (1966) 1009 –1015.
22. S. Muslov, A. Lotkov, V. Timkin, Calculation of Poisson's Ratios of TiNi Shape Memory Crystals through Their Elastic Constants, AIP Conf. Proc. 2310 (2010) 020215.
23. K. Li, M. Li, Ya. Zhao, W. Shan, Yu. Cao, D. Guo, Achieving ultralow elastic modulus in TiNi alloy by controlling nanoscale martensite phase, Mater. Lett. 233 (2018) 282 – 285.
24. V. Brailovski, S. Prokoshkin, P. Terriault, F. Trochu (Eds.), Shape Memory Alloys: Fundamentals, Modeling and Applications, École de technologie supérieure (ETS), Université du Québec, CANADA, Montreal, 2003, 844 p.